

Energy transfer in adsorption. I. Experiments*

Ch. Steinbrüchel and L. D. Schmidt

Department of Chemical Engineering and Materials Science, University of Minnesota, Minneapolis, Minnesota 55455

(Received 13 June 1974)

The angle-dependent sticking coefficients $s(\phi)$ of H_2 , D_2 , N_2 , CO , and CO_2 on $W(100)$ and $W(110)$ have been measured as a function of the angle of incidence ϕ using a simple molecular-beam apparatus. In general, $s(\phi)$ increases slightly towards grazing incidence, as predicted by classical models based on condensation via momentum transfer to the substrate. However, for H_2 and D_2 on $W(110)$, $s(\phi)$ decreases markedly towards grazing incidence. For these systems, measurements of $s(\phi)$ and the total sticking coefficient s as functions of gas and surface temperature have also been carried out. The experimental results are discussed briefly in terms of various mechanisms of energy transfer from the gas to the substrate.

INTRODUCTION

Rates of condensation are probably the most widely varying and least understood processes in chemisorption. Condensation rates (measured by the sticking coefficient or probability of condensation s) are frequently observed to vary by several orders of magnitude between different metals or different crystal planes of the same metal.¹ The theoretical interpretation of such processes is complicated by the fact that most data are obtained by exposing the surface to an isotropic gas flux, i. e., s represents an average over all incident angles. Molecular-beam techniques have been used extensively to probe the angular dependence of gas-surface interactions,² but most of these studies were concerned with the scattering of noble gases from surfaces. With adsorbing gases, only a few beam experiments have been carried out, in which either inferences on condensation were made from observations on the scattered portion of the beam³⁻⁵ or a beam was used as a gas-dosing device.⁶ King and Wells,⁷ in an experiment similar to ours, found no angular dependence of the sticking coefficient of N_2 on polycrystalline tungsten.

In this paper, we report measurements of angle-dependent sticking coefficients $s(\phi)$ as a function of angle of incidence ϕ with respect to the surface normal on two single-crystal planes of W . We are also able to measure the dependence of $s(\phi)$ and s on gas temperature over a wide range as well as on surface temperature. We find a small angular dependence of $s(\phi)$ for most gases and crystal planes. This is in qualitative agreement with classical models of condensation via momentum transfer to the lattice. For hydrogen on the (110) plane, we observe behavior which is in qualitative disagreement with these notions. Extensive measurements of the dependence of $s(\phi)$ on ϕ , gas and surface temperatures, and adsorbate mass have been made for this system in an effort to

understand the mechanisms of energy transfer in condensation. A preliminary account of these results has appeared previously,⁸ and details of model calculations of condensation will be presented in a subsequent paper.⁹

EXPERIMENTAL

Apparatus

The apparatus consisted of a Pyrex ultrahigh-vacuum chamber (Fig. 1) with ancillary gas-handling and electronic equipment. Total pressures in chambers A and B were measured with Bayard-Alpert ion gauges. The composition of the background gas in the reaction chamber B was monitored with a quadrupole mass spectrometer. At low pressures, the system was pumped primarily by a tantalum film getter pump with a measured pumping speed of ~ 80 liter/sec. A mercury diffusion pump, backed by a mechanical pump, was used for the initial pumpdown. After baking the system at $\sim 300^\circ C$, out-gassing all metal filaments, and depositing a tantalum getter, an ultimate pressure of $\sim 6 \times 10^{-10}$ Torr was attained in B .

A molecular beam was formed by gas effusing from a capillary 1 mm in diameter and 25 mm long. This directed gas flux impinged on a single-crystal disk (~ 6 mm in diameter, ~ 0.3 mm thick) positioned ~ 7 cm from the capillary. The crystal had been cut from a high-purity single-crystal tungsten rod and polished such that both faces were within 1° of the stated orientation. The edges of the (110) crystal were cut such that they also exposed (110) planes in order to minimize errors that might be introduced by the presence of other planes on a circular edge. The crystal was mounted on a metal holder and could be rotated with an external magnet. The incident angle ϕ between the normal to the crystal surface and the beam could be determined visually to $\pm 2^\circ$.

The geometry of the beam-crystal arrangement

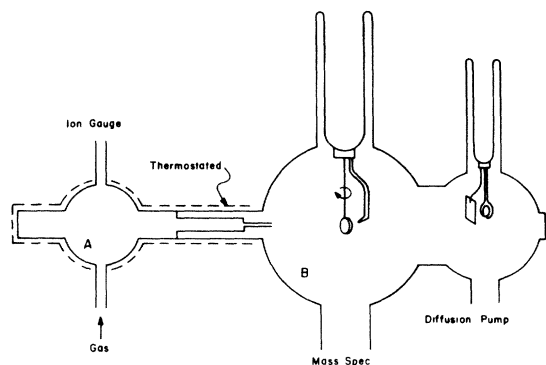


FIG. 1. Schematic diagram of vacuum system.

was such that at all incident angles the crystal was exposed to a uniform gas flux with negligible angular divergence. The angle formed between the crystal and the opening of the capillary was $\sim 5^\circ$ so that the angle of incidence varied by $\pm 2.5^\circ$ or less over the crystal surface. The flux per unit area was estimated to vary by $< 4\%$ across the crystal at $\phi = 0^\circ$. The proper alignment of the crystal was further checked by noting that amounts adsorbed due to the beam were measured to be independent of whether the crystal was rotated clockwise or counterclockwise with respect to the beam.

The crystal could be heated to 2500°K by electron bombardment. It could also be cooled with dry ice or liquid N_2 in the Dewar on top of chamber B (Fig. 1). The temperature of the molecular beam was varied by either heating the walls of chamber A with a heating tape, or by cooling them with dry ice. The wall temperature was measured to be uniform to within $\pm 5^\circ\text{K}$.

Procedure

The crystals were cleaned by heating to 2500°K in ultrahigh vacuum and to 1600°K in O_2 at 10^{-7} Torr. Separate experiments using Auger-electron spectroscopy have shown that such procedures produce surfaces free of contamination.^{10,11} Flash desorption spectra of H_2 and CO at saturation from both surfaces reproduced those reported in the literature and confirmed the cleanliness of the surface.^{10,12-15}

Before each experimental run, gases adsorbed from the background were removed by flashing the crystal to 2500°K several times. With the background pressure $P_B \leq 1 \times 10^{-9}$ Torr, a steady-state gas flux through the capillary was established ($P_A \sim 5 \times 10^{-6}$ Torr). This raised P_B to $\sim 2 \times 10^{-9}$ Torr. Amounts adsorbed in a fixed time interval, typically 200 sec, were measured as a function of ϕ by flash desorption.¹⁶ Flash desorption spectra were taken with the mass spectrometer and recorded on a storage oscilloscope, using a high-

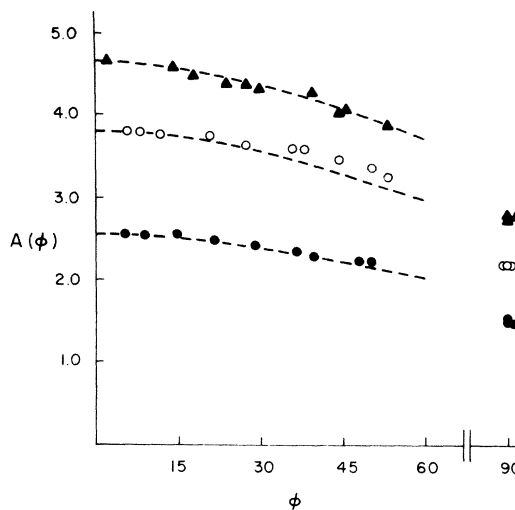


FIG. 2. Typical data of amount adsorbed, $A(\phi)$ vs incident angle ϕ , for CO on W(110). Dashed lines represent curves for which $A(\phi) - A(90^\circ) \propto \cos \phi$, i. e., $s(\phi) = \text{const}$. $T_g = T_s = 300^\circ\text{K}$.

speed electrometer amplifier. The pump-out time for the system was typically < 0.1 sec, and the time interval over which gas desorbed from the crystal was ~ 1 sec. Hence, the observed pressure burst was proportional to the rate of desorption, and the amount of gas adsorbed was proportional to the area under the corresponding peak in the flash desorption spectrum.¹⁶ Coverages were always so small ($\theta < 0.2$) that only the most tightly-bound state was populated.

RESULTS

A typical example of amount adsorbed $A(\phi)$ vs ϕ is shown in Fig. 2 for CO on W(110). Under the conditions described above, $A(90^\circ)$ is due to the isotropic background, and hence, $A(\phi) - A(90^\circ)$ is proportional to $s(\phi) \cos \phi$. [The angular variation of amounts adsorbed on the edges of the

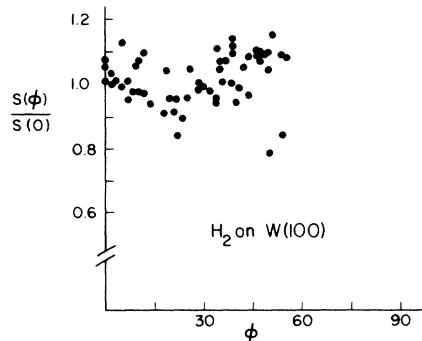


FIG. 3. Data for $s(\phi)/s(0)$ of H_2 on W(100). $T_g = T_s = 300^\circ\text{K}$.

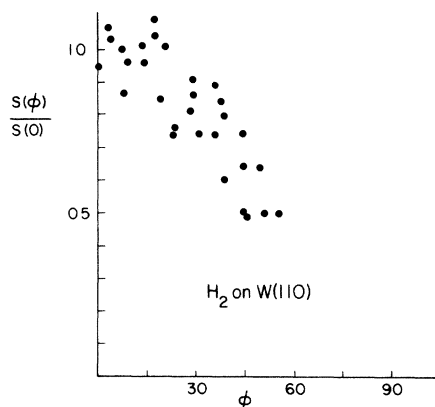


FIG. 4. Data for $s(\phi)/s(0)$ of H_2 on $W(110)$. $T_g = T_s = 300^\circ K$.

crystal was estimated to be less than 3% of $A(90^\circ)$ and was corrected for.]. Since the data for $A(\phi) - A(90^\circ)$ did not deviate greatly from a curve proportional to $\cos\phi$ (cf. Fig. 2), they were fit to an expression of the form $a \cos(\phi) + b \cos(3\phi)$. Thus, one obtains

$$s(\phi) = s(0)(1 + \epsilon \sin^2 \phi), \quad (1)$$

with $\epsilon = -4b/(a+b)$ and $s(0) = a+b$. In Figs. 3 and 4 are displayed $s(\phi)/s(0)$ data for H_2 on $W(100)$ and $W(110)$. For $\phi > 60^\circ$, $A(\phi) - A(90^\circ)$ could not be determined accurately because of the relatively large background contribution.

In Table I are shown average values for ϵ , calculated from 50 to 100 data points, together with their statistical errors. Figures 5 and 6 show the corresponding curves for $T_s = 300^\circ K$ and $T_g = 300^\circ K$. The errors of the curves for H_2 are

TABLE I. Variations of $s(\phi)$ with angle of incidence on tungsten.

Plane	Gas	T_g ($^\circ K$)	T_s ($^\circ K$)	ϵ^a
(100)	H_2	300	300	$+0.02 \pm 0.06$
	N_2			$+0.15 \pm 0.09$
	CO			$+0.16 \pm 0.14$
	CO_2			-0.05 ± 0.07
(110)	H_2	300	300	-0.71 ± 0.11
	D_2			-0.79 ± 0.14
	CO			-0.13 ± 0.09
	H_2	195	300	-0.56 ± 0.09
		375		-0.80 ± 0.10
		468		-0.91 ± 0.05
	D_2	468		-0.98 ± 0.10
	H_2	300	78	-0.71 ± 0.09

^aValues of ϵ , calculated from experimental data, for various gases on the (100) and (110) planes of tungsten. $s(\phi) = s(0)(1 + \epsilon \sin^2 \phi)$.

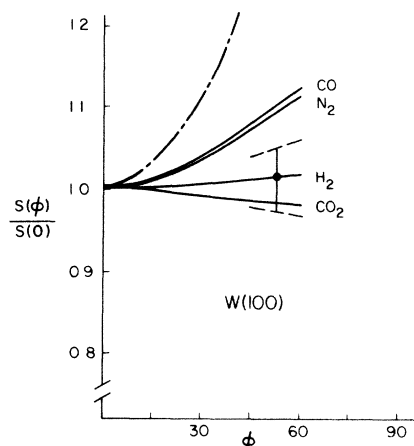


FIG. 5. Curves for $s(\phi)/s(0)$ on $W(100)$ fit to experimental data. $T_g = T_s = 300^\circ K$. Dashed lines indicate error limits of H_2 curve. Dashed-dotted curve is calculated for CO according to the classical square-well model.

indicated by dashed lines. We note that $s(\phi)$ is constant or increases slightly with increasing ϕ except for H_2 and D_2 on $W(110)$, where $s(\phi)$ decreases sharply with increasing ϕ . The result for CO_2 on $W(100)$ further confirms that the crystal was properly aligned with the beam since $s \approx 1$ for CO_2 on $W(100)$,¹⁴ and therefore, $s(\phi)$ should not vary with ϕ .

In order to elucidate further the surprising behavior of H_2 and D_2 on $W(110)$, measurements were taken at different gas and surface temperatures. The results are summarized in Table I. Figure 7 shows $s(\phi)/s(0)$ as a function of T_g with $T_s = 300^\circ K$ for H_2 and D_2 on $W(110)$. There is a

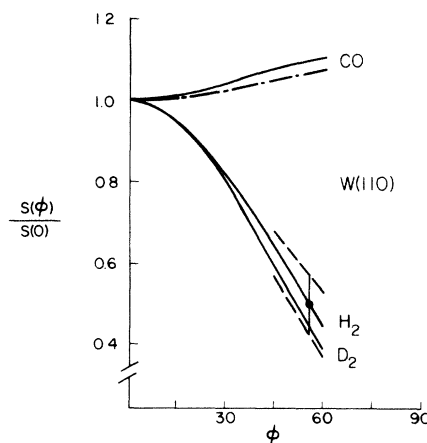


FIG. 6. Curves for $s(\phi)/s(0)$ on $W(110)$ fit to experimental data. $T_g = T_s = 300^\circ K$. Dashed lines indicate error limits of H_2 curve. Dashed-dotted curve is calculated for CO according to the classical square-well model.

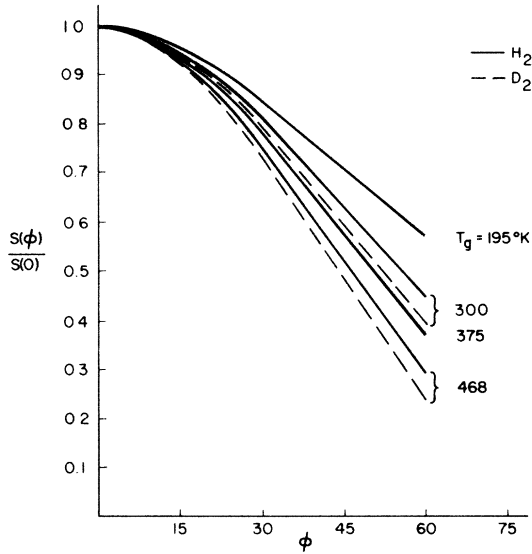


FIG. 7. Curves fit to experimental data showing gas temperature dependence of $s(\phi)/s(0)$ for H_2 and D_2 on $W(110)$. $T_s = 300^\circ K$.

definite trend for $s(\phi)/s(0)$ to become more peaked as T_g increases. Again, the curves for H_2 and D_2 are within the error limits of each other. Furthermore, for H_2 at $T_g = 300^\circ K$, $s(\phi)/s(0)$ is the same at $T_s = 78^\circ K$ as it is at $T_s = 300^\circ K$ (cf. Table I).

It is also possible to estimate the total sticking coefficient s as a function of T_g if the form of $s(\phi)$ as given in Eq. (1) is assumed to be valid up to 90° . Then

$$s = 2 \int_0^{\pi/2} s(\phi) \sin\phi \cos\phi d\phi = s(0)(1 + \frac{1}{2}\epsilon), \quad (2)$$

where $s(0)$ and ϵ both depend on T_g .⁹ The dependence of $s(0)$ on T_g is determined from the experimental data as follows. Let $B(\phi)$ be the amount adsorbed due to the beam in a fixed time interval [$B(\phi) = A(\phi) - A(90^\circ)$], and let $B'(\phi)$ be the corresponding flash desorption signal. If upon admission of the beam the pressures in A and B increase by ΔP_A and ΔP_B to P_A and P_B , respectively (Fig. 1), then the flux f in molecules sec^{-1} due to the beam into chamber B is

$$f = (kT_g)^{-1} \frac{4}{3} \bar{v}_g \Delta P_A q, \quad (3)$$

where \bar{v}_g is the mean speed of the gas molecules and q is a geometrical factor given by the dimensions of the capillary. From Eq. (3), f is proportional to $\Delta P_A (T_g m)^{-1/2}$ where m is the mass of a gas molecule. On the other hand, in the steady state

$$f = (kT_B)^{-1} \Delta P_B \frac{dV_B}{dt}, \quad (4)$$

where V_B is the volume of chamber B . From Eq. (1), $B'(0) = a + b$. In addition, $B'(0) \propto B(0) S^{-1}$, where $S = dV_B/dt$ is the pumping speed in chamber B . Furthermore, $B(0)$ is equal by definition to the beam flux onto the crystal times $s(0)$, i. e., $B(0) \propto s(0) P_A (T_g m)^{-1/2}$. Hence, we have

$$a + b \propto s(0) P_A (T_g m)^{-1/2} S^{-1}. \quad (5)$$

Using Eqs. (3)–(5) and the fact that T_B is constant in all cases, it follows that

$$s(0) \propto (a + b) P_A^{-1} \Delta P_A / \Delta P_B. \quad (6)$$

The total sticking coefficient s as a function of T_g for H_2 on $W(110)$ with $T_s = 300^\circ K$ is displayed in Fig. 8. $s(T_g = 300^\circ K)$ was set equal to 0.07, the value reported previously by Tamm and Schmidt.¹⁷ In Fig. 8, we also give two values of s for D_2 . In order to determine these values, the sensitivities of the mass spectrometer for H_2 and D_2 were calibrated by setting equal the areas under the flash desorption spectra at saturation. (Saturation amounts must be the same for H_2 and D_2). We note from Fig. 8 that s decreases with increasing T_g for both gases.

Figure 8 further shows that $s_{D_2}/s_{H_2} \approx 1$ at $T_g = 300^\circ K$ and $468^\circ K$. This result confirms previous measurements of relative sticking coefficients of H_2 and D_2 on $W(100)$ and $W(110)$ from a uniform background.¹⁸ Those experiments indicated that $s_{D_2}/s_{H_2} \approx 1.4$ on $W(100)$, but $s_{D_2}/s_{H_2} \approx 1.0$ on $W(110)$.

Of course one can also use Eq. (6) to compare s at different T_s . It is found that for H_2 on $W(110)$ at $T_g = 300^\circ K$, $s(T_s = 300^\circ K)/s(T_s = 78^\circ K) = 1.36$

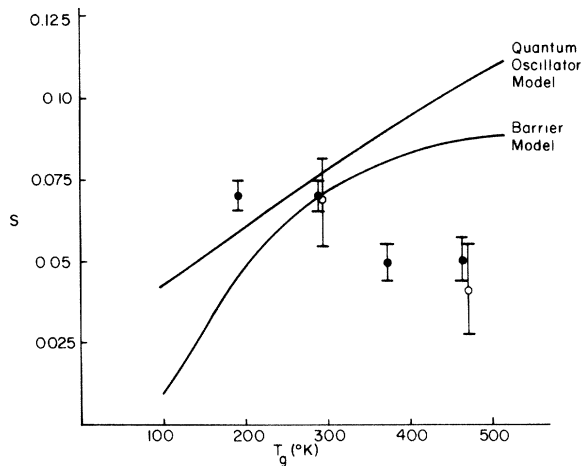


FIG. 8. Data on gas temperature dependence of total sticking coefficient s for H_2 and D_2 on $W(110)$. Also shown are forms of $s(T_g)$ as predicted by the barrier and quantum oscillator models.

± 0.18 . Thus, s appears to increase slightly with increasing T_g .

DISCUSSION

We examined previously the predictions on $s(\phi)$ of a classical model in which the gas-surface potential was assumed to be a one-dimensional square well and the gas-surface collision was represented by the collision between an atom and a harmonic oscillator.¹⁹ With well depths of the order of a few kcal/mole, the model yields qualitatively the correct dependence of s on T_g .¹⁹ The model also predicts that $s(\phi)$ should in general increase towards grazing incidence, particularly for light gases. This angular dependence is intuitively reasonable since the number of molecules having a normal momentum that is sufficiently small to lead to trapping increases towards grazing incidence. These model predictions agree fairly well with our data for the heavier gases (CO, N₂, CO₂), but not for H₂ and D₂ (cf. Figs. 5 and 6).

The surprising decrease of $s(\phi)$ towards grazing incidence for H₂ and D₂ on W(110) suggests that condensation does not occur via simple classical momentum transfer to the lattice. The fact that $s(\phi)$ is lower at grazing incidence, where less energy needs to be transmitted for condensation, implies some sort of threshold for the transfer of energy from the gas to the surface. We have tried to simulate this threshold in two different ways: by including a barrier in the gas-surface potential and by taking the surface oscillator to be quantized.⁹ The forms of $s(\phi)$ resulting from these two models are shown in Fig. 9. We note that both models give $s(\phi)$ decreasing towards grazing incidence, with the quantum oscillator model reproducing the shape of $s(\phi)$ fairly well. The quantum oscillator model also yields the proper dependence of $s(\phi)$

on T_g , whereas the barrier model does not. However, neither model describes the measured dependence of s on T_g .⁹ The two models also predict that $s_D/s_H \approx 1.5$, which is in disagreement with our data on the (110) plane (cf. Fig. 8).

We have also considered the contributions to trapping by mechanisms other than momentum transfer from the gas to the lattice of the solid.⁹ It is not clear in what way internal degrees of freedom of the gas molecules, particularly rotation, affect trapping. On the other hand, energy transfer via direct excitation of substrate electrons seems to become generally less efficient towards grazing angles of incidence. This is because molecules with smaller normal momenta penetrate the repulsive part of the gas-surface potential less deeply and hence should interact less strongly with the substrate electrons.

SUMMARY

It appears from these rather limited data that, except for very light gases on the close-packed planes, sticking coefficients do not vary significantly with the angle of incidence of the gas molecules, and that $s(\phi)$ generally increases toward grazing incidence as predicted by simple classical theories of condensation via momentum transfer to the lattice. It should also be noted that the angle of incidence dependence of $s(\phi)$ will probably be smaller for more open planes [the (110) and (100) planes are the highest density planes of W] because the gas-surface potential should be less uniform on these planes.

For hydrogen on the (110) plane, the data suggest the existence of some sort of threshold which makes condensation more efficient for a large perpendicular component of momentum. The three simple models we have considered—a potential energy barrier, quantization of phonon production, and excitation of substrate electrons—are all capable of predicting a decrease in $s(\phi)$ near grazing incidence, but none simultaneously gives the observed dependence of s on m or T_g . It is certainly possible that this is due to the inadequacies of the models, but it is difficult to see why their qualitative predictions should be incorrect if the representative mechanisms were operative. Of course, several mechanisms of energy transfer could be in effect simultaneously, and there is then no reason to assume that their contributions would be strictly additive. There is a need for additional measurements of angular dependences of sticking coefficients on other surfaces such as the fcc metals, the variations with adsorbate coverage, and for detailed calculations of gas-surface potentials and the sticking coefficients predicted with these potentials.

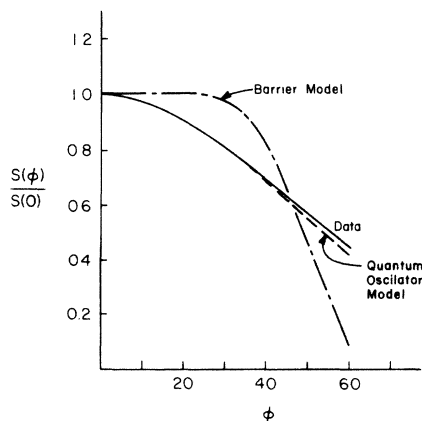


FIG. 9. Comparison of $s(\phi)/s(0)$ data for H₂ on W(110) with best fits according to the barrier and quantum oscillator models.

- *Partially supported by National Science Foundation under Grant No. GK16241.
- ¹L. D. Schmidt, in *Adsorption-Desorption Phenomena*, edited by F. Ricca (Academic, New York, 1972), p. 391.
- ²H. Saltsburg, *Annu. Rev. Phys. Chem.* 24, 493 (1973).
- ³R. Chappell and D. O. Hayward, *J. Vac. Sci. Technol.* 9, 1052 (1972).
- ⁴R. Sau and R. P. Merrill, *Surf. Sci.* 34, 268 (1973).
- ⁵R. L. Palmer and J. N. Smith, Jr., *J. Chem. Phys.* 60, 1453 (1974).
- ⁶T. E. Madey, *Surf. Sci.* 36, 281 (1973).
- ⁷D. A. King and M. E. Wells, *Surf. Sci.* 29, 454 (1972).
- ⁸Ch. Steinbrüchel and L. D. Schmidt, *Phys. Rev. Lett.* 32, 594 (1974).
- ⁹Ch. Steinbrüchel and L. D. Schmidt, following paper, *Phys. Rev. B* 10, 4215 (1974).
- ¹⁰Y. Viswanath and L. D. Schmidt, *J. Chem. Phys.* 59, 4184 (1973).
- ¹¹R. W. Joyner, J. Rickman, and M. W. Roberts, *Surf. Sci.* 39, 445 (1973).
- ¹²P. W. Tamm and L. D. Schmidt, *J. Chem. Phys.* 51, 5352 (1969).
- ¹³P. W. Tamm and L. D. Schmidt, *J. Chem. Phys.* 54, 4775 (1971).
- ¹⁴L. R. Clavenna and L. D. Schmidt, *Surf. Sci.* 33, 11 (1972).
- ¹⁵C. Kohrt and R. Gomer, *Surf. Sci.* 24, 77 (1971).
- ¹⁶P. A. Redhead, *Vacuum* 12, 203 (1962).
- ¹⁷P. W. Tamm and L. D. Schmidt, *J. Chem. Phys.* 55, 4253 (1971).
- ¹⁸S. M. Ko, Ch. Steinbrüchel, and L. D. Schmidt, *Surf. Sci.* 43, 521 (1974).
- ¹⁹Ch. Steinbrüchel and L. D. Schmidt, *J. Phys. Chem. Solids* 34, 1379 (1973).